The Journal of Immunology

The Class III Kinase Vps34 Promotes T Lymphocyte Survival through Regulating IL-7Rα Surface Expression

Ian X. McLeod, Xiang Zhou, Qi-Jing Li, Fan Wang and You-Wen He

J Immunol 2011; 187:5051-5061; Prepublished online 21 October 2011;
doi: 10.4049/jimmunol.1100710
http://www.jimmunol.org/content/187/10/5051

The Journal of Immunology is published twice each month by
The American Association of Immunologists, Inc.,
1451 Rockville Pike, Suite 650, Rockville, MD 20852

Print ISSN: 0022-1767 Online ISSN: 1550-6606.

The Class III Kinase Vps34 Promotes T Lymphocyte Survival through Regulating IL-7Rα Surface Expression

Ian X. McLeod,* Xiang Zhou,† Qi-Jing Li,* Fan Wang,† and You-Wen He*

IL-7Rα–mediated signals are essential for naive T lymphocyte survival. Recent studies show that IL-7Rα is internalized and either recycled to cell surface or degraded. However, how the intracellular process of IL-7Rα trafficking is regulated is unclear. In this paper, we show that Vps34, the class III PI3K, plays a critical role in proper IL-7Rα intracellular trafficking. Mice lacking Vps34 in T lymphocytes had a severely reduced T lymphocyte compartment. Vps34-deficient T lymphocytes exhibit increased death and reduced IL-7Rα surface expression, although three major forms of autophagy remain intact. Intracellular IL-7Rα in normal T lymphocytes at steady state is trafficked through either early endosome/multivesicular bodies to the late endosome-Golgi for surface expression or to the lysosome for degradation. However, Vps34-deficient T cells have mislocalized intracellular Eea1, HGF-regulated tyrosine kinase substrate, and Vps36 protein levels, the combined consequence of which is the inability to mobilize internalized IL-7Rα into the retromer pathway for surface display. Our studies reveal that Vps34, though dispensable for autophagy induction, is a critical regulator of naive T cell homeostasis, modulating IL-7Rα trafficking, signaling, and recycling. ***The Journal of Immunology*****, 2011, 187: 5051–5061.**

Naive T lymphocytes are maintained by multiple homeostatic mechanisms involving TCR signaling, cytokines, and nutrient factors (1). IL-7 is a central cytokine for naive T lymphocyte survival by promoting multiple antiapoptotic pathways (2). IL-7, produced mainly by stromal elements in secondary lymphoid organs, is unique, since its production is not dependent on exogenous signals, but is kept at constant levels (3). Thus, usage of this cytokine must be enforced on a cell autonomous basis through the regulation of IL-7R expression. The IL-7R consists of IL-7Rα, and the common γ-chain that is also shared by type 1 cytokines (4). The responsiveness of T lymphocytes to IL-7 is regulated primarily by IL-7Rα because the common γ is expressed ubiquitously (2, 3).

Much work has been done to study the regulation of IL-7Rα expression at the transcriptional level (2, 5). Robust IL-7 signaling induces downregulation of IL-7Rα mRNA transcription (6). IL-7–induced downregulation of IL-7Rα on T lymphocytes is thought to be an important homeostatic mechanism to ensure the maximal survival of naive T cells in an IL-7–limited environment.

Recent studies have demonstrated that IL-7Rα is also subjected to posttranslational regulation. IL-7Rα is internalized under steady state and upon IL-7 stimulation through clathrin-mediated endocytosis (7). Although some of the internalized IL-7Rα is degraded in a proteasome- and lysosome-dependent manner, a significant fraction of the internalized IL-7Rα recycles back to the cell surface, which is essential to maintain proper IL-7Rα surface expression (7, 8). However, how IL-7Rα trafficking is completed intracellularly and what molecules regulate this key process remain unknown.

Along with IL-7Rα–mediated signaling, several other mechanisms exist to ensure T cell homeostasis. Autophagy, a highly conserved intracellular process, has been identified as a novel mechanism regulating T lymphocyte homeostasis (9, 10). T lymphocytes lacking the autophagy gene *Atg5* or *Atg7* undergo large-scale apoptosis and exhibit defective intracellular mitochondria clearance, increased reactive oxidative species (ROS) level, and impaired proliferation (9, 11). The autophagy pathway is carried out primarily through two ubiquitin-like conjugation systems that consist of 33 different autophagy-related genes in yeast and mammals (12). Among them, the sole class III PI3K *Vps34* has been shown to play a critical role in the initiation of autophagy in yeast and higher organisms (13, 14). Specifically, in *Saccharomyces cerevisiae*, Vps34 mutants had defective turnover of late Golgi proteins after rapamycin treatment (14). In addition, in HT-29 adenocarcinoma cells, knockdown of hVps34 led to a decrease in long-lived protein turnover (13). Vps34 has a single substrate specificity, phosphorylating the 3-hydroxylposition on phosphatidylinositol, which in turn acts as a localization signal recruiting many proteins with Fab-1, YGL023, Vps27, and EEA1 (FYVE) or GRAM-like-ubiquitin-binding in EAP45 (GLUE) domains. Vps34 is anchored to membranes by its myristoylated interaction partner, Vps15 (15), and is localized to several endomembranes, including endosomes, multivesicular bodies (MVB), and endoplasmic reticulum (16). Interaction between Vps15 and Vps34 has been shown to increase the activity of Vps34. Vps34 functions in two major complexes, both involving the tumor suppressor Beclin-1 (14, 17, 18). The first complex, involving UVRAG and Atg14L, has been proposed to function in autophagy induction (19). The second complex, involving Rubicon, seems to downregulate autophagy and control endosomal sorting functions (20). The

*Department of Immunology, Duke University Medical Center, Durham, NC 27710; and †Department of Cell Biology, Duke University Medical Center, Durham, NC 27710

Received for publication March 14, 2011. Accepted for publication September 9, 2011.

This work is supported by National Institutes of Health Grants AI074944 and AI074754 (to Y.-W.H.).

Address correspondence and reprint requests to Prof. You-Wen He, Department of Immunology, Box 3010, Duke University Medical Center, Durham, NC 27710. E-mail address: he000004@mc.duke.edu

The online version of this article contains supplemental material.

Abbreviations used in this article: DP, double positive; DN, double negative; ESCRT, endosomal sorting complex required for transport; FYVE, Fab-1, YGL023, Vps27, and EEA1; GLUE, GRAM-like-ubiquitin-binding in EAP45; HRS, HGF-regulated tyrosine kinase substrate; MVB, multivesicular body; PI(3)P, phosphatidylinositol 3-phosphate; ROS, reactive oxidative species; SP, single positive; TEM, transmission electron microscopy; WT, wild-type.

association of Vps34 with Beclin-1 is important to recruit proteins that have membrane-flexing qualities, such as Bif-1, to induce curvature of expanding vesicles (21). Taken together, Vps34 plays a complex role in signaling and recruitment of effectors for vesicle formation and endomembrane trafficking, as well as autophagic induction in several systems (22, 23).

In studying the role of Vps34 in T lymphocytes, we have found that Vps34 is essential for T lymphocyte development and survival. Most surprisingly, the critical role of Vps34 for T cell survival is independent of autophagy. Rather, Vps34 regulates IL-7Rα expression by directing its proper intracellular trafficking at multiple steps. Our results have identified a key molecular regulator for IL-7Rα surface expression in T lymphocytes and mapped out a route for normal IL-7Rα intracellular trafficking.

Materials and Methods

Mice

Vps34-deficient T lymphocytes were generated by crossing Vps34-floxed mice (24) to Lck-Cre transgenic mice (The Jackson Laboratory). Genomic deletion was assessed by PCR detection of the Vps34-floxed allele (5′-AACTGGATCTGGGCCTATG-3′ [forward] and 5′-CACTCACCTGCTGTGAAATG-3′ [reverse]) and Vps34-deleted allele (5′-AACTGGATCTGGGCCTATG-3′ [forward] and 5′-GAAGCCTGGAACGAGAAGAG-3′ [reverse]). $Bim^{-/-}$ mice were purchased from The Jackson Laboratory, and $hBcl2^{+}$ transgenic mice were a gift from Dr. M. Kondo (Duke University). All mice were bred and housed in Duke's specific pathogen-free facilities in accordance with Institutional Animal Care and Use Committee regulations.

Abs and reagents

FITC, PE, PE-cy5, allophycocyanin, APC-cy7, or Pacific Blue-conjugated anti-CD3, -CD4, -CD8, -CD44, -CD62L, –IL-7RA, -B220, -QA2, –IL-2, -CD132, -CD71, -pStat5(Y694), -Stat5, and –Bcl-2 were purchased from BioLegend, eBioscience, and BD Pharmingen. Anti-LC3 (PD015), -p62, and Z-VAD-FMK were purchased from MBL. Anti-Vps34 was purchased from Abgent. Anti-HRS was purchased from Abnova. Anti-TGN46, -Vps35, and -Vps36 were purchased from Abcam. Recombinant murine IL-7 was purchased from PeproTech. Fluorokine biotin–human IL-7 was purchased from R&D Systems.

Flow cytometry

Single-cell suspensions with RBCs lysed were incubated with FcR blocker (2.4G2; eBioscience) and were immunostained for all surface markers. For intracellular staining, cells were fixed in 4% paraformaldehyde for 20 min, washed, and permeabilized in 0.1% saponin for 20 min. All stains were performed in 0.1% saponin thereafter. All FACS used a BD Facscanto II (BD Biosciences, Franklin Lakes, NJ).

Cell proliferation

Total single-cell suspensions of splenocytes or lymphocytes at 10^7/ml were stained in 5% FBS at 5 μM CFSE (Molecular Probes) for 5 min and washed three times. Cells were stimulated with soluble anti-CD3 at 5 μg/ml and anti-CD28 at 2 μg/ml for 48 or 72 h.

Mitochondrial content and ROS production

Mitotracker Green (Molecular Probes), dihydroethidium (Sigma-Aldrich), and CM-H_2DCFDA (Molecular Probes) were used as described previously (11).

Electron microscopy

Mature lymph node T cells after EasySep-negative bead selection (StemCell Technologies) were Ab stained and lightly fixed in 1% paraformaldehyde. One million $CD4^+$ T cells were sorted and fixed in a 4% glutaraldehyde and 0.1 M sodium cacodylate buffer overnight. The samples were rinsed in 0.1 M cacodylate buffer containing 7.5% sucrose three times for 15 min each and fixed in 1% osmiumin cacodylate buffer for 1 h. After being washed three times in 0.11 M veronal acetate buffer for 15 min each, the samples were incubated with 0.5% uranyl acetate in veronal acetate buffer for 1 h at room temperature. Specimens were then dehydrated in an ascending series of ethanol (35, 70, 95, and two changes of 100%) for 10 min each, followed by two changes of propyleneoxide for 5 min each. The samples were incubated with a 1:1 mixture of 100% resin and propylene oxide for 1 h, followed by two changes of 100% resin, each for 30 min. Finally, the samples were embedded in resin and polymerized at 60°C overnight. Thick sections (0.5 μm) were cut and stained with toluidine blue for light microscopy selection of the appropriate area for ultrathin sections. Thin sections (60–90 nm) were cut, mounted on copper grids, and poststained with uranyl acetate and lead citrate. Micrographs were taken with a Philips LS 410 electron microscope. Images were analyzed using AxioVision software (Zeiss).

Fluorescence microscopy

All images were captured with a custom-built Zeiss Observer D1 using a Zeiss ×100 objective lens and a 1.4 numerical aperture. Images were captured using a Photometrics Cool SNAP HQ2 and analyzed using Metamorph software for punctae number, size, and intensity. Images were deconvoluted and thresholded, and colocalization was determined using Autoquant ×2 software. Deconvolution was done blind at 40 iterations. Flurochromes used included Pacific Blue, Cy3, FITC, and Cy5. γ Value adjustments were made to CD127-linked flurophores to 1.25 for ease of viewing in comparison with other fluorophores.

Statistical analysis

All statistical analysis was performed using Prism software (GraphPad Software). Tests for cell numbers, death assays, LC-3, HRS, IL-7Rα punctae formation and recovery, mitochondrial content, and ROS levels were paired, two-tailed Student *t* tests.

Results

Reduced T lymphocyte compartment in Vps34-conditional knockout mice

To investigate the role of Vps34 in T lymphocyte development and function, we ablated Vps34 kinase activity in T cells by crossing mice containing loxP sites flanking exons 17 and 18 of Vps34 (24) to a Cre recombinase under the control of the Lck regulatory elements (25). Exons 17 and 18 correspond to the ATP-binding domain ofVps34, which were replaced by a premature stop codon. We first examined thymocyte development in Vps34-deficient mice. All four subsets of thymocytes as defined by CD4 and CD8 expression were detected in Vps34-deficient mice. However, the total thymic cellularity was reduced by >50% in Vps34-deficient mice with drastic reductions in both the $CD4^+CD8^+$ double positive (DP) and $CD4^+$or $CD8^+$ single positive (SP) compartments (Fig. 1*A*, 1*B*). Although the double negative (DN) percentage was increased in $Vps34_{f/f}$Lck-cre thymocytes, none of the populations was significantly increased, and because DN1 and DN2 thymocytes should not yet express the Lck promoter-driven recombinase, this difference was likely due to thymic architecture and not inherent thymocyte defects (Supplemental Fig. 1*A*). Interestingly, there was a clear gene-dosage effect as $Vps34^{f/+}$Lck-cre heterozygote mice had a significant reduction ($p < 0.05$) in the numbers of DP, $CD4^+$, and $CD8^+$ SP thymocytes (Fig. 1*B*). We also found that $Qa2^+CD4^+$ SP or $Qa2^+CD8^+$ SP mature T cells were much reduced (Fig. 1*C*).

We next examined the peripheral T lymphocyte compartment in $Vps34^{f/f}$Lck-cre mice. The number of $CD4^+$and $CD8^+$ T cells in the spleen and lymph nodes of $Vps34^{f/f}$Lck-cre mice were reduced by >80% (Fig. 1*D*, 1*E*). These cells expressed comparable levels of CD3 to that on wild-type (WT) T cells (Fig. 1*D*). Similar to the thymus, Vps34 haploinsufficiency was observed for both $CD4^+$ and $CD8^+$ T cell compartments (Fig. 1*D*, 1*E*). As expected in a lymphopenic environment, the number of T cells with an activated/memory/homeostatic proliferation phenotype was increased in T cells lacking one or both copies of Vps34 (Fig. 1*D*).

The peripheral T cells in Vps34-deficient mice may be composed of cells that have escaped Lck-Cre–mediated deletion. $CD4^+$ peripheral T lymphocytes had almost undetectable expression of Vps34 by fluorescence microscopy, and genomic deletion of Vps34 was maximal in animals up to 6 wk of age (Supplemental

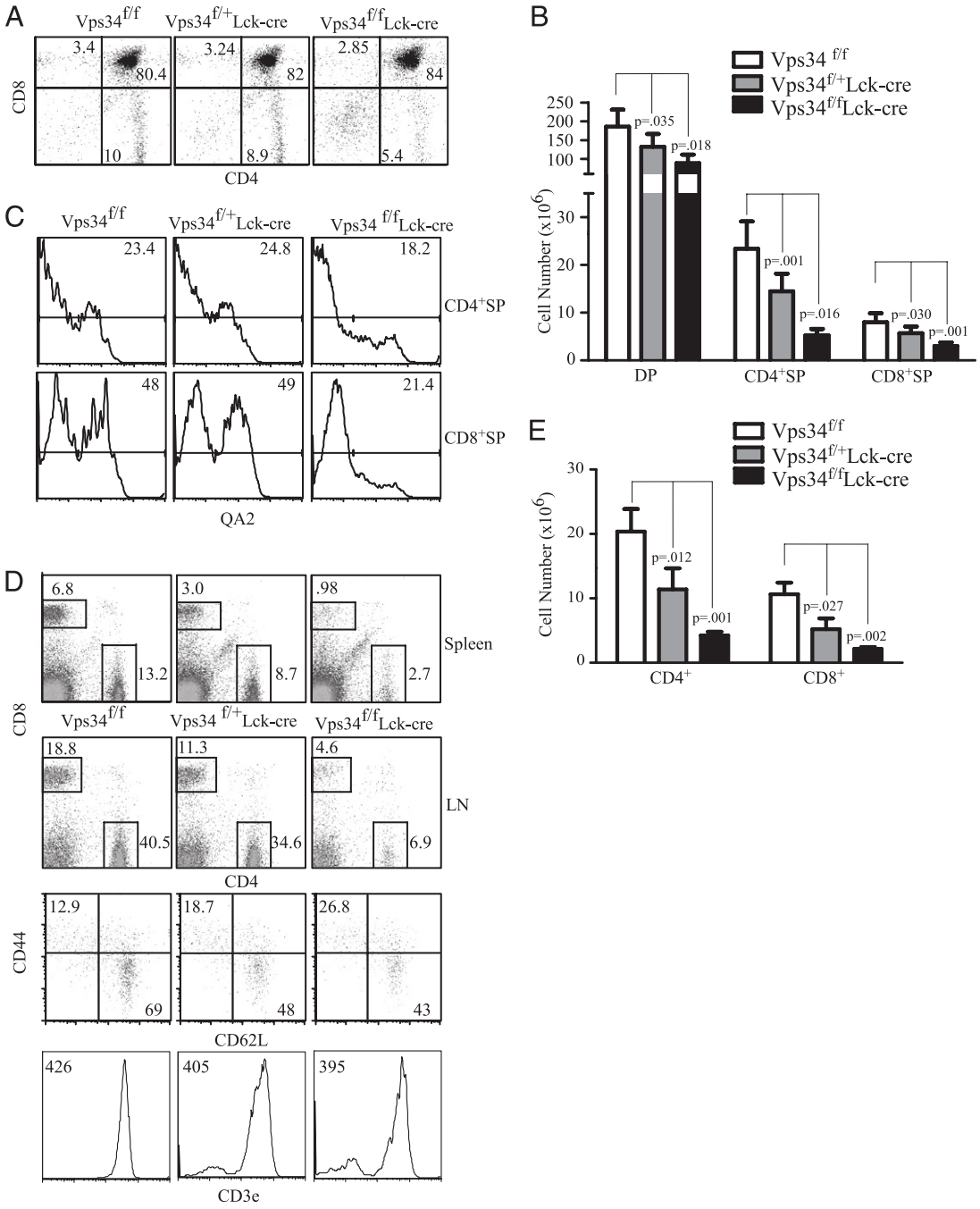

FIGURE 1. Phenotypic analysis of Vps34$^{f/f}$Lck-cre T cells. *A*, Thymic profile of Vps34$^{f/f}$Lck-cre andVps34$^{f/+}$Lck-cre null mice that were 5.5–6 wk old. *B*, Cell numbers from thymi of Vps34$^{f/f}$Lck-cre mice. The *p* values are shown; $n = 12$. *C*, QA2 expression in CD4$^+$ or CD8$^+$ SP thymocytes of Vps34$^{f/f}$Lck-cre mice. *D*, T cell profiles of spleen and lymph nodes from 6-wk-old mice of control and Vps34$^{f/f}$Lck-cre mice. *E*, Cell numbers of mature CD4$^+$ or CD8$^+$ T cells in Vps34$^{f/f}$Lck-cre mice. The *p* values are shown; $n = 12$.

Fig. 1*B*, 1*C*). Also, deletion of Vps34 assessed by Western blot showed that Vps34 was 75% deleted in CD4SP thymocytes and in excess of 80% in mature, naive CD4-lineage T cells (Supplemental Fig. 1*B*). Interestingly, Vps34 protein was only minimally deleted in DP thymocytes, which reflects the very long half-life of Vps34 protein. Alternatively, it is possible that DP cells, which have lost Vps34 protein expression earlier in the DP stage, are committed to apoptosis, whereas thymocytes that lose Vps34 expression later, for example, while in the DP-to-SP transition are viable to complete thymic development.

The mature, active/memory CD4$^+$ T cells had minimal deletion of Vps34 and represent a population that has escaped deletion, although the genomic deletion is still clean from the total mature CD4 population. All experiments were subsequently performed using naive cells exclusively. Taken together, these results demonstrate that Vps34 plays an essential role for the survival of developing T lymphocytes. Taken together, these results demonstrate that Vps34 plays an essential role for the survival of developing T lymphocytes.

Vps34-deficient T cells succumb to apoptosis

The impaired T lymphocyte compartment in Vps34-deficient mice was similar to that in mice lacking other autophagy genes, Atg5 or Atg7 (9, 11). Autophagy-deficient T cells readily undergo apoptosis. To determine whether Vps34$^{f/f}$Lck-cre T cells had increased apoptosis, we first stained freshly isolated T cells from

these mice. Deletion of Vps34 in thymocytes and peripheral T cells resulted in a >2-fold increase in apoptosis of these cells (Fig. 2*A*). To further characterize the defect of Vps34$^{f/f}$Lck-cre T cells, we examined the survival of Vps34$^{f/f}$Lck-cre SP thymocytes and peripheral CD44^{low}naive T cells in vitro culture with or without IL-7 or the caspase inhibitor zVAD. Vps34$^{f/f}$Lck-cre CD4$^+$or CD8$^+$ naive T cells did not respond to IL-7, whereas WT T cells survived well in the presence of IL-7 (Fig. 2*B*). However, Vps34$^{f/f}$Lck-cre CD4 T lymphocytes showed a modest but significant improvement in survival in the presence of zVAD (Fig. 2*B*). In addition, the administration of other common γ-chain cytokines, IL-4 and IL-15, gave no significant increase in the survival of Vps34$^{f/f}$Lck-cre T cells, despite supporting WT T cells (Supplemental Fig. 2*G*). These results suggest that an important function of Vps34 is to promote T lymphocyte survival. Given that the number of naive CD8$^+$ T cells was very low in Vps34$^{f/f}$Lck-cre mice and that many of these cells had either escaped deletion or were CD8$^+$ cells of a non-T lineage, we focused our following analysis on CD4$^+$ T cells.

Normal autophagy induction in Vps34-deficient T cells

Similar to autophagy-deficient T cells (Atg5- or Atg7-null), Vps34$^{f/f}$ Lck-cre T cells exhibited reduced number and increased apoptosis. Because Vps34 has been shown to be critical in autophagy induction in almost all organisms and cells types investigated (16, 26), we tested whether there were any discernable defects in several forms of autophagy induction inVps34$^{f/f}$Lck-cre T cells. Autophagy is induced in T lymphocytes by stimulation through

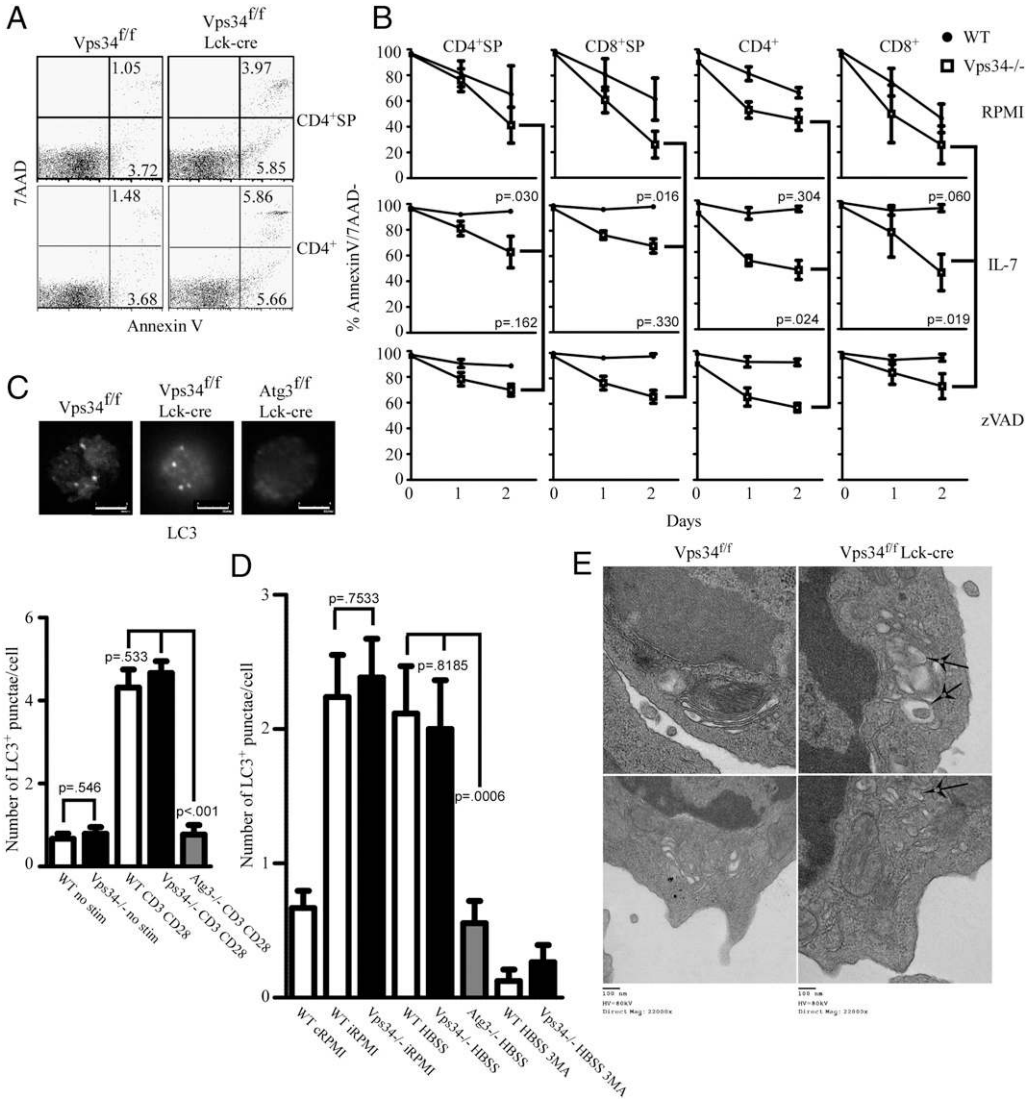

FIGURE 2. Enhanced apoptosis but normal autophagy in Vps34-deficient T cells. *A*, Apoptosis staining of freshly isolated control and Vps34$^{f/f}$Lck-cre T cells from 6-wk-old mice. *B*, Increased apoptosis of Vps34$^{f/f}$Lck-cre T cells in vitro culture. Cells were cultured in RPMI 1640 medium alone or with IL-7 (1 ng/ml) or zVAD (20 μM). Peripheral cells were gated on CD44^{low} populations, and Annexin V/7-aminoactinomycin D (7AAD) exclusion was measured at 0, 24, and 48 h. Shown are mean and SD from four individual experiments. The *p* values provided correspond to complete RPMI 1640 medium compared with IL-7 treatment and IL-7 treatment compared with zVAD treatment. *C*, Activation-induced autophagy in Vps34$^{f/f}$Lck-cre T cells. Forty-eight hours after anti-CD3/CD28 stimulation, control, Vps34$^{f/f}$Lck-cre, and Atg3-deficient CD4$^+$ cells were stained with anti-LC3 Ab and quantified for LC3 punctae formation by microscopy. Shown are representative pictures of the LC3 staining. A total of 30 cells were counted and shown. *D*, Starvation-induced autophagy. Sixteen hours poststarvation, autophagy was measured in the indicated cells under different culture media. A total of 30 cells were quantified. *E*, TEM of Vps34$^{f/f}$Lck-cre CD4$^+$ T cells. *Left panels* are representative of WT T cells with ordered Golgi stacks and budding vesicles. *Right panels* are representative of Vps34$^{f/f}$Lck-cre T cells with asymmetric vesicle traffic but intact autophagosomes. Arrows indicate autophagosomal structures in Vps34$^{f/f}$ Lck-cre T cells. A total of 25 cells from each genotype have been examined with TEM. Scale bars, 100 nm. High voltage (HV) of the electron beam = 80 kV. Original magnification ×22,000.

the TCR complex (9). We stimulated WT and Vps34$^{f/f}$Lck-cre naive CD4$^+$ T cells with anti-CD3 plus anti-CD28 and examined LC-3 punctae formation. Although there was a significant increase in cell death in the TCR-stimulated Vps34$^{f/f}$Lck-cre T cells (data not shown), live cells were sorted after 48 h of stimulation and analyzed for LC3 mobilization by fluorescence microscopy. Qualitatively, these punctae had various sizes and varied in their cytoplasmic location considerably (Fig. 2*C*). However, there was no quantitative difference in the number of punctae between activated WT andVps34$^{f/f}$Lck-cre T cells (Fig. 2*C*). Sorted, activated T lymphocytes from an Atg3$^{f/f}$Lck-cre (Atg3$^{-/-}$) were used as a negative control for induction. We next examined starvation-induced autophagy. Because many Vps34$^{f/f}$Lck-cre T cells are committed to apoptosis by 24 h, we examined shorter starvation periods. Naive CD4$^+$ T lymphocytes were withdrawn from serum (incomplete RPMI 1640) or amino acids (HBSS) for 16 h and cultured in vitro. Cells were then stained for LC3, and punctae were quantified. Consistent with TCR stimulation-induced autophagy, no defect in starvation-induced autophagy in Vps34$^{f/f}$Lck-cre T cells was found (Fig. 2*D*). LC3 processing assessed by Western blot was also normal in T cells lacking Vps34 (Supplemental Fig. 2*D*). In T lymphocytes, amino acid withdrawal (HBSS) did not seem to induce autophagy to levels over that of serum withdrawal (iRPMI) but was readily inhibited by the addition of 5 mM 3-methyladenine (Fig. 2*D*). Finally, we investigated the basal levels of autophagy in Vps34$^{f/f}$Lck-cre T cells using transmission electron microscopy. Although many abnormal vesicles were present in naive Vps34$^{f/f}$Lck-cre lymphocytes, autophagosomes, with characteristic double membrane-bound morphology and cytoplasmic contents, were clearly observed (Fig. 2*E*). When both electron scarce double membrane-bound structures (autophagosomes) and electron dense structures (lysosomes) were quantified in WT and Vps34 T cell cross-sections, no difference was observed, indicating that autophagy initiation was not only intact in the absence of Vps34, but maturation of autolysosomes appeared to be normal as well (Supplemental Fig. 2*F*). Thus, no obvious defects in the three major forms of autophagy (basal, TCR, and starvation-induced) in T cells were observed in Vps34$^{f/f}$Lck-cre T cells.

Autophagy-deficient T lymphocytes exhibit several other important defects including impaired clearance of mitochondria, increased production of ROS, and an inability to proliferate upon TCR stimulation (9, 11). However, Vps34$^{f/f}$Lck-cre T cells had comparable levels of mitochondria and ROS to those in WT T cells (Supplemental Fig. 2*A*, 2*B*), indicating that both mitophagy and pexophagy are intact in maintaining the intracellular redox state in the absence of Vps34. Furthermore, Vps34$^{f/f}$Lck-cre T cells had equal proliferative capacity to WT T cells from littermate controls (Supplemental Fig. 2*C*). Finally, to measure autophagic flux of a specific substrate, we measured the levels of p62 (SQSTM1), which is selectively degraded during autophagy. In fresh Vps34$^{f/f}$Lck-cre CD4 T cells, levels of p62 were slightly higher than WT controls, and this difference was more pronounced 6 h after TCR stimulation. However, 20 h poststimulation, Vps34$^{f/f}$Lck-cre T cells had efficiently downregulated p62 to WT levels, which were considerably lower than p62 levels in resting T cells (Supplemental Fig. 2*E*). Collectively, these results demonstrate that Vps34 is not required for autophagic initiation or substrate inclusion into autophagosomes in T lymphocytes.

Decreased Bcl-2 expression in Vps34f/fLck-cre T cells

A potential explanation for the defective survival of Vps34$^{f/f}$Lck-cre T cells could be altered levels of Bcl-2 family members. Bcl-2 and Mcl-1 are crucial for the survival of naive T lymphocytes in vivo (27). We examined Bcl-2 levels in CD4$^+$ SP thymocytes and naive T cells lacking Vps34 by intracellular staining. The levels of Bcl-2 in CD4$^+$ T cells from Vps34$^{f/f}$Lck-cre mice were

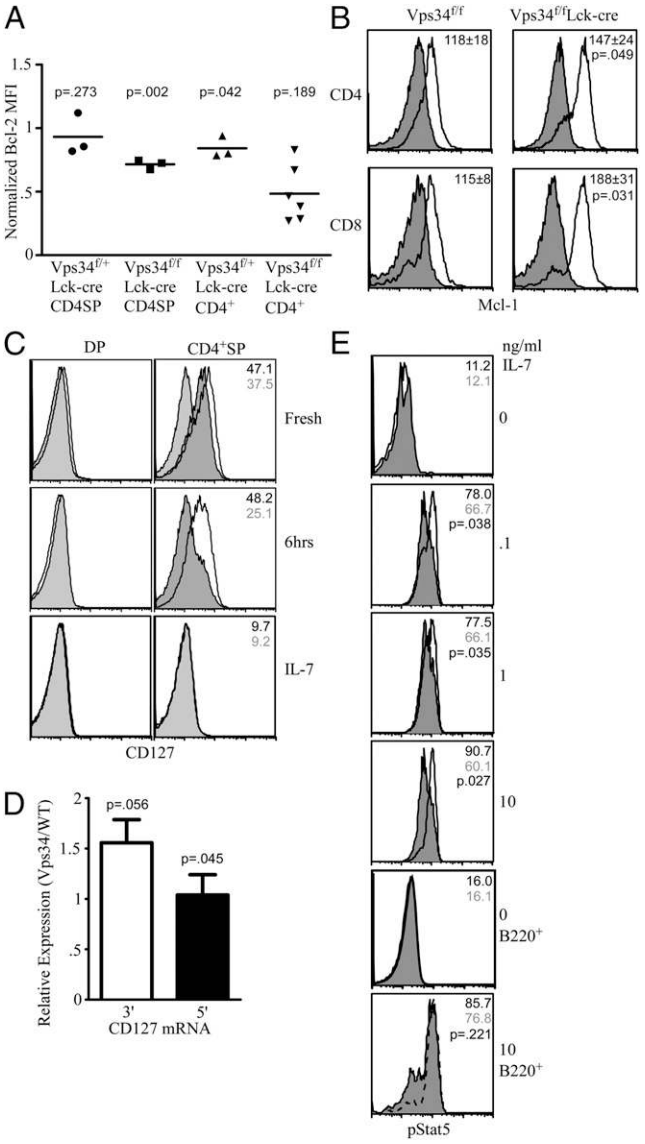

FIGURE 3. Impaired IL-7Rα expression and signaling in Vps34$^{f/f}$Lck-creT cells. *A*, Levels of Bcl-2 protein in Vps34$^{f/f}$Lck-cre T cells. Intracellular Bcl-2 staining of Vps34$^{f/f}$Lck-creT cells was normalized to that of WT T cells ($n \geq 3$).Student *t* tests compare the mean fluorescence intensities (MFIs) of the Bcl-2 levels to those of the WT controls before normalization. *B*, Intracellular staining of Mcl-1 in Vps34$^{f/f}$Lck-cre T cells. Shaded histograms represent Ig-matched isotype controls. *C*, IL-7Rα expression on Vps34$^{f/f}$Lck-cre thymocytes. IL-7Rα surface expression was examined on CD4$^+$ SP thymocytes that were freshly isolated, starved for 6 h in HBSS, or incubated with rIL-7 (5 ng/ml) for 6 h. Numbers represent the MFIs of indicated proteins. *D*, IL-7Rα mRNA expression in Vps34$^{f/f}$Lck-cre T cells. Freshly isolated naive CD4$^+$ T cells from WT and Vps34$^{f/f}$Lck-cre mice were measured for IL-7Rα mRNA expression with two primer sets, one 5′ and one 3′, and normalized to β-actin. Student *t* tests compare the mRNA levels to those of the WT controls before normalization. *E*, IL-7 induced Stat5 phosphorylation in Vps34$^{f/f}$Lck-cre T cells. Naive CD4$^+$ T cells were stimulated with IL-7 and assessed for Stat5 phosphorylation by intracellular staining. Student *t* tests compare the pStat5 MFIs of Vps34$^{f/f}$Lck-cre T cells under each stimulation condition to the corresponding WT MFI. Numbers indicate MFIs of pStat5. *C* and *E*, Unshaded histograms represent WT T cells, dark grey histograms represent Vps34$^{f/f}$ Lck-cre T cells, and lightly shaded histograms are isotype controls. All data are representative of three experiments unless otherwise specified.

reduced by 30–80% (Fig. 3*A*). The Bcl-2 level was also slightly reduced in Vps34$^{f/+}$Lck-cre CD4$^+$ naive T cells (Fig. 3*A*). Interestingly, Mcl-1 expression level was higher in Vps34$^{f/f}$Lck-cre T cells than that in control T cells (Fig. 3*B*). These results are in contrast to those observed in Atg7-deficient T cells that Bcl-2 expression level was 2-fold higher, whereas Mcl-1 expression was not altered compared with control T cells (11). These data suggest that the reduced Bcl-2 expression levels may cause the survival defect of Vps34$^{f/f}$Lck-cre T cells.

Impaired IL-7Rα dynamics in Vps34$^{f/f}$Lck-cre T cells

One place that Vps34 may mediate its effect is on intracellular sorting. Because Vps34 is localized largely to early endosomes, multivesicular bodies, and the Golgi (18, 28), and Vps34$^{f/f}$Lck-cre T cells have reduced survival and Bcl-2 expression, we hypothesized that Vps34 may regulate homeostatic sorting of prosurvival cytokine receptor(s) in T lymphocytes. IL-7/IL-7R interaction provides critical survival signals to naive T cells (2), and recent data suggest that IL-7Rα is internalized, and a fraction of the internalized receptor recycles back to the surface on human T lymphocytes (7, 8). To investigate whether Vps34 regulates IL-7Rα surface display, we examined IL-7Rα levels on freshly isolated WT and Vps34$^{f/f}$Lck-cre thymocytes or CD4$^+$naive T cells. Interestingly, IL-7Rα levels on Vps34$^{-/-}$CD4$^+$ SP thymocytes or naive T cells were lower than WT controls (Figs. 3*C*, 5*A*). In these experiments, DP thymocytes were used as a baseline, because they express very little IL-7Rα, indistinguishable from isotype controls. When thymocytes were placed in media without exogenous IL-7, Vps34$^{f/f}$Lck-cre CD4$^+$ SP thymocytes were unable to maintain IL-7Rα expression (Fig. 3*C*). However, Vps34$^{f/f}$Lck-cre CD4$^+$ SP thymocytes efficiently downregulated IL-7Rα surface expression upon IL-7 stimulation (Fig. 3*C*).The reduced IL-7Rα surface expression in Vps34$^{f/f}$Lck-cre T cells was not due to reduced mRNA of IL-7Rα (Fig. 3*D*). These results demonstrate that IL-7Rα internalization and transcription are not impaired.

To test the functional consequence of impaired IL-7Rα surface expression, we examined Stat5 phosphorylation in Vps34$^{f/f}$Lck-cre T cells. Lymphocytes from Vps34$^{f/f}$Lck-cre and WT littermate control mice were starved for 6 h and cultured with various doses of rIL-7 for 20 min. Cells were fixed, and levels of phosphorylated Stat5 were measured. Phosphorylation of Stat5 in Vps34$^{f/f}$Lck-cre CD4$^+$ lymphocytes in response to IL-7 was impaired, and the defect could not be overcome by a high level of IL-7 (10 ng/ml) (Fig. 3*E*). B220$^+$ B cells present in the same sample served as positive control had a maximal upregulation of phosphorylated Stat5 (Fig. 3*E*). Taken together, these results demonstrate that Vps34 regulates IL-7Rα surface expression in T lymphocytes through a transcription independent mechanism.

Disrupted IL-7Rα intracellular trafficking in Vps34$^{f/f}$Lck-cre T lymphocytes

Given the defective IL-7Rα surface expression dynamics and Vps34's previous description as an inducer of autophagy as well as normal lysosomal trafficking, we examined the intracellular structure of Vps34-deficient T cells by TEM. In WT T cells, vesicular structure was ordered and symmetric (Fig. 2*E*), with clear endoplasmic reticulum and Golgi structures. Vesicles budding off the endoplasmic reticulum were visible, as were autophagic vacuoles. In contrast, the vesicles in Vps34-deficient T cells were completely entropic and asymmetric, suggesting a defect in vesicle maturation and efficient trafficking (Fig. 2*E*).

Recent studies suggest that IL-7Rα is constitutively internalized via clathrin-coated pits, and the internalization is increased upon IL-7 stimulation (7). Upon internalization, a fraction of IL-7Rα is degraded, whereas a significant fraction recycles back to the cell surface. We tested IL-7Rα intracellular trafficking and degradation using fluorophore-labeled rIL-7. When added to in vitro cultures of primary T lymphocytes, WT naive CD4$^+$ lymphocytes efficiently took up the IL-7, and over a period of 20 h, gradually degraded the fluorophore signal (Fig. 4*A*, 4*B*), presumably via thelysosome and proteasome (7, 8). However, although Vps34-deficient T cells only took up ~50% of the amount of labeled IL-7 and some only had background levels of the cytokine (Fig. 4*A*), by 4 h, the amount of labeled IL-7 on these cells was equal to that on control T cells on a per cell basis (Fig. 4*B*). By 20 h, all the initially bound IL-7 was still present in Vps34$^{f/f}$Lck-cre T cells (Fig. 4*A*, 4*B*). In contrast, B220$^+$ cells from Vps34$^{f/f}$Lck-cre mice took up similar levels of IL-7 (Fig. 4*A*) and degraded the cytokine within 20 h (data not shown). These results suggest that Vps34$^{f/f}$ Lck-cre T cells had a defect in proper trafficking of the cytokine–receptor complex, so it cannot recycle back to the cell surface or traffic to degradative compartments.

The inability to respond to cytokine was specific to IL-7Rα, because CD132 was expressed normally on Vps34$^{f/f}$Lck-cre T cells at all stages of development (Fig. 4*C*). CD132 has a very simple trafficking pattern. After signaling and endocytosis, it is targeted to late endosomes and degraded by lysosomes (29). The differential effect on IL-7Rα and CD132 expression on Vps34$^{f/f}$Lck-cre T cells suggests that IL-7Rα is regulated in a different manner. We have also tested the receptor levels for several other cell surface markers, some of which have known kinetics and trafficking patterns. We measured the expression of these markers in permeabilized and nonpermeabilized cells. CD3, CD25 (IL-2Rα), and TCRβ, which all have very rapid recycling patterns dependent on early endosomal function, as well as CD124 (IL-4Rα), CD5, and $\alpha_4\beta_7$ integrin, all had identical expression regardless of Vps34 expression (Supplemental Fig. 3). These results suggest that the defective IL-7Rα expression on Vps34$^{f/f}$Lck-cre T cells is not due to a global defect in cell surface receptor expression.

A significant proportion of IL-7Rα is intracellular

To further investigate the regulation of IL-7Rα intracellular trafficking by Vps34, we measured the levels of IL-7Rα before and after permeabilization of control andVps34$^{f/f}$Lck-cre T cells. When T cells were permeabilized, the levels of IL-7Rα were doubled from cell surface staining (Fig. 5*A*). In Vps34$^{f/f}$Lck-cre T cells, the levels of intracellular IL-7Rα (total staining minus cell surface staining) were comparable to those in WT T cells (Fig. 5*A*). When compared with WT T cells, the proportion of membrane-bound IL-7Rα in Vps34$^{f/f}$Lck-cre T cells was reduced by 60–70% (Fig. 5*B*). Because MVB are a major subcellular sorting site, and several ESCRT subunits have either FYVE or GLUE domains, both of which bind PI(3)P (30, 31), these organelles were quantified. Although the expression levels of the GLUE domain-containing HGF-regulated tyrosine kinase substrate (HRS), an ESCRT-0 coreprotein, were similar in Vps34$^{f/f}$ Lck-cre T cells (Fig. 5*C*), the size of the MVB as measured by HRS volume under fluorescence microscopy was vastly increased (Fig. 5*D*). We next examined the expression levels of Vps35, a retromer subunit, responsible for retrograde translocation of postendocytic components back to the Golgi for surface expression, and Vps36, a GLUE domain-bearing ESCRT-II subunit that can bind ubiquitinated proteins. The expression levels of Vps35 and Vps36 in Vps34$^{f/f}$Lck-cre T cells were increased (Fig. 5*E*). These results suggest that MVBsin Vps34$^{f/f}$Lck-cre T cells are less dynamic and have a deficiency in maturing toward either Golgi or lysosomal compartments.

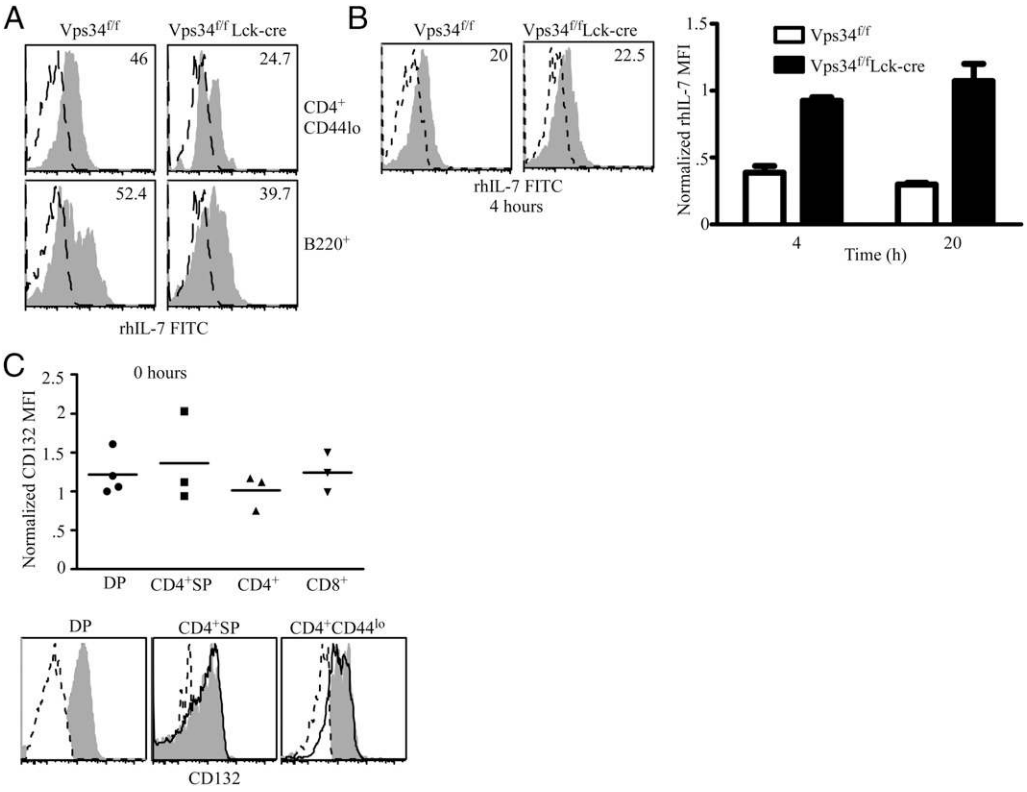

FIGURE 4. Altered IL-7R dynamics in Vps34$^{f/f}$Lck-cre T cells. *A*, Uptake of FITC-conjugated recombinant human (rh)IL-7 in freshly isolated, nonpermeabilized, control, and Vps34$^{f/f}$Lck-creCD4$^+$ T cells. B cells were used as controls. *B*, IL-7 degradation in Vps34$^{f/f}$Lck-cre T cells. FITC–rhIL-7 was measured on control and Vps34$^{f/f}$Lck-cre T cells at 4 and 20 h. Data were normalized to the mean fluorescence intensity of bound and internalized rhIL-7 on these T cells at 0 h. *C*, Expression of CD132 on the surface of freshly isolated Vps34$^{f/f}$Lck-cre T cells. Data are representative of three experiments.

Vps34 localizes to MVB to promote IL-7Rα recycling via Vps36-containing vesicles

To investigate the role of Vps34 in MVB sorting in T lymphocytes, naive CD4$^+$ T cells were stained with Vps34 and HRS. There was a consistent colocalization between the two markers, indicating that Vps34 localizes to early-stage MVB in T lymphocytes (Fig. 6*A*).However, there was little colocalization between IL-7Rα and HRS (Fig. 6*A*). Much of the IL-7Rα localized in compartments in close proximity to the Golgi enzyme mannosidase (Fig. 6*B*). This brings up the possibility that intracellular IL-7Rα trafficking requires a retrograde transport to the Golgi for surface re-expression. Because Vps34$^{f/f}$Lck-cre T cells had increased MVB size (Fig. 5*D*), we hypothesized that Vps34$^{f/f}$Lck-cre T cells have impaired inward vesiculation mediated by ESCRT proteins. With the ESCRT-II proteinVps36 as a marker, which contains a GLUE domain, WT and Vps34$^{f/f}$Lck-cre T cells were costained for IL-7Rα and TGN46, a *trans*-Golgi marker. A majority of the punctate intracellular IL-7Rα colocalized with Vps36 in WT T cells, but not in Vps34$^{f/f}$Lck-cre T cells (Fig. 6*C*, 6*D*). We hypothesize that Vps36 needs PI(3)P for proper localization to mediate the inward vesiculation of IL-7Rα containing vesicles from the MVB. Consistent with results seen in Fig. 6*B*, a significant portion of both IL-7Rα and Vps36 also localized to the Golgi in WT but not Vps34$^{f/f}$Lck-cre T cells (Fig. 6*C*). This suggests that IL-7Rα requires MVB to Golgi sorting for proper recycling.

To further investigate the possibility of a retrograde endosome to Golgi recycling event necessary for optimal IL-7Rα surface expression, naive CD4$^+$ T cells were starved for 2 h and costained for Vps35 and IL-7Rα. Vps35 is involved in the retromer complex that has been shown to mediate retrograde transport of early- or late-endosomal cargos for secretion or surface re-expression (32), which would otherwise be degraded in the late-endosomal to lysosomal pathway (33). A significant portion of intracellular IL-7Rα colocalized with Vps35 positive compartments (Fig. 6*E*), although not nearly as well as with Vps36. Very little IL-7Rα was observed colocalizing with Vps35 in the absence of Vps34. This observation is consistent with previous data that at steady state some internalized IL-7Rα is not recycled (8).

Defective IL-7Rα recovery in Vps34$^{f/f}$Lck-cre T cells

To investigate the kinetics of IL-7Rα surface expression in the absence of Vps34, pronase was administered to purified naive CD4$^+$ cells and the recovery of surface IL-7Rα was measured as described previously (34). In short, this proteinase was administered to T cells to cleave surface receptors, and the cells were allowed to recover in media for the indicated time points. The receptor was detectable on the surface of WT cells within 2 h postcleavage and reached peak levels by 6 h under starvation conditions (Fig. 7*A*). However, Vps34$^{f/f}$Lck-cre T cells had minimal recovery up to 6 h postcleavage and not until 8 h posttreatment did a majority of IL-7Rα recover (Fig. 7*A*). The recovery of IL-7Rα surface expression was inhibited by the microfilament polymerization inhibitor, cytochalasin B, up to 4 h postpronase treatment (Fig. 7*B*, 7*C*). However, addition of the protein biosynthesis inhibitor cycloheximide, had minimal effect on IL-7Rα recovery in WT T cells until 6 h posttreatment (Fig. 7*B*, 7*C*). These results suggest that naive T cells have an intracellular store of IL-7Rα sufficient to withstand at least several hours of starvation without the need to translate new protein. Such a mechanism would allow naive T cells to rapidly adapt autonomously to changes in local cytokine concentration, perhaps even by polarizing receptor surface display toward higher local concentrations.

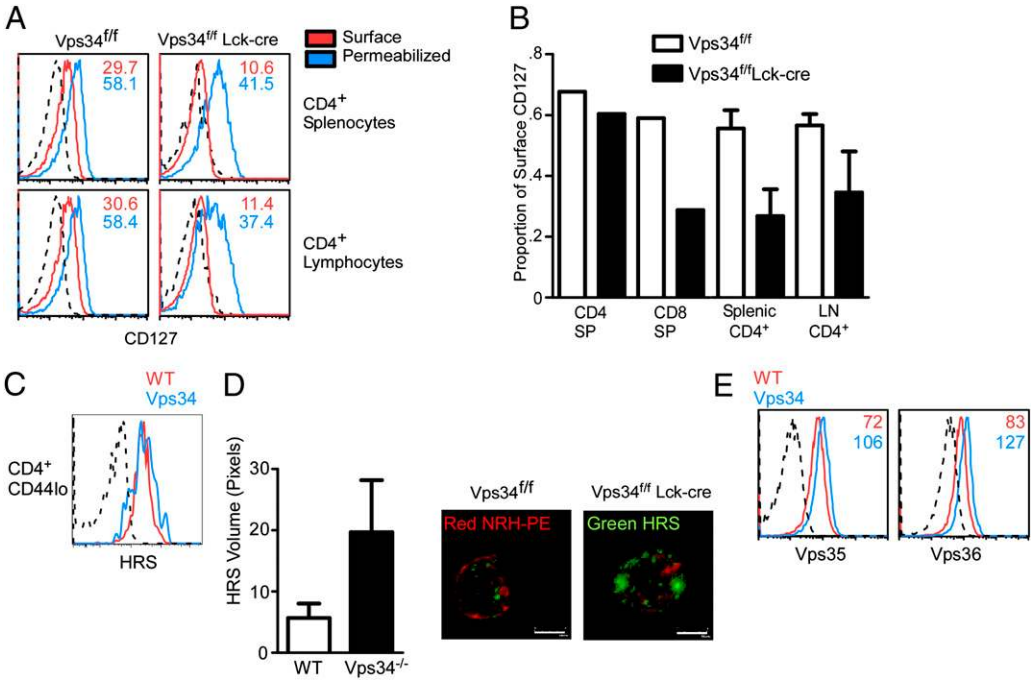

FIGURE 5. Intracellular trafficking of IL-7Rα in Vps34$^{f/f}$Lck-cre T cells. *A*, IL-7Rα expression in permeabilized (blue) or surface (red) stained freshly isolated CD4^{+}CD44^{lo} T cells in WT andVps34$^{f/f}$Lck-cre T lymphocytes. Numbers indicate mean fluorescence intensities of IL-7Rα. *B*, Proportion of surface IL-7Rα expression in Vps34$^{f/f}$Lck-cre T cells. The results are derived from staining shown in *A* from four experiments. *C*, Expression of HRS, an ESCRT-0 protein, in WT and Vps34$^{f/f}$Lck-cre T cells. Intracellular staining of HRS was measured by FACS. *D*, Average volume of HRS-containing MVB in WT and Vps34$^{f/f}$Lck-cre T cells as measured by fluorescence microscopy. N-rhodamine-labeled phosphatidylethanolamine (NRH-PE) was used to label endocytotic vesicles and normalize HRS fluorescence. *E*, Expression of Vps35 (retromer subunit) andVps36 (ESCRT-II subunit) in Vps34$^{f/f}$Lck-cre T cells. Intracellular staining of Vps35 and Vps36 was performed on WT and Vps34$^{f/f}$Lck-creT cells. Accumulation of these proteins indicates lack of MVB maturation in the absence of Vps34. Dotted lines in *A*, *C*, and *E* are isotype-matched Ab control. Data are representative of three experiments. *C–E*, Vps34 = Vps34$^{f/f}$Lck-cre.

In contrast, Vps34$^{f/f}$Lck-cre T cells have minimal ability to mobilize intracellular IL-7Rα and must rely on de novo synthesized receptor at later time points, putting them at a disadvantage.

Bcl-2 can partially rescue Vps34 deficiency

Given that Vps34$^{f/f}$Lck-creT cells have defective survival, reduced IL-7Rα, and Bcl-2 expression, we asked whether genomic deletion of several proapoptotic Bcl-2 family members or overexpression of Bcl-2 itself could rescue Vps34 deficiency in T lymphocytes. Deletion of Bim, a BH3-only proapoptotic protein that is induced upon cytokine withdrawal, had no effect on Vps34 deficiency (Supplemental Fig. 4*A*). Similarly, deletion of Bax did not rescue the survival defectof Vps34$^{f/f}$Lck-cre T cells (data not shown). However, the expression of a human Bcl-2 transgene (35) significantly promoted early Vps34$^{f/f}$Lck-cre T cell survival at the CD4^{+} SP lineage (Supplemental Fig. 4*B*, 4*C*). These results suggest that the defective survival of Vps34$^{f/f}$Lck-cre T cells is not solely due to a reduced expression of Bcl-2.

Discussion

PI3Ks consist of three classes and play important roles in a wide variety of cellular functions (36). Although extensive studies have been performed on the function of class I and II PI3Ks, relatively little is known about the specific function of Vps34, the sole class III PI3K in mammals in vivo. By specifically deleting Vps34 in T lymphocytes, we have found that Vps34 is essential for thymocyte survival and naive T lymphocyte homeostasis. Vps34 regulates T cell homeostasis by promoting their survival via cell surface expression of IL-7Rα. It is clear that IL-7Rα is regulated at both the transcriptional and posttranslational level. IL-7Rα is continuously internalized for recycling and degradation. Our results have mapped out a detailed route for IL-7Rα intracellular trafficking that is critically regulated by Vps34 at multiple points.

Although Vps34 is critical for autophagy induction in other types of cells (13, 14), our data demonstrate that it is not required for autophagy induction in T lymphocytes. This conclusion is supported by our findings that three major forms of autophagy including TCR-induced, starvation, and basal level autophagy in Vps34$^{f/f}$Lck-cre T cells are comparable to those in WT T lymphocytes. In addition, the turnover of an autophagy-specific substrate, p62/SQSTM1, is normal in Vps34$^{f/f}$Lck-cre T cells. Importantly, there are significant differences on the phenotypes exhibited by autophagy-deficient (Atg5$^{-/-}$or Atg7$^{f/f}$Lck-cre) and Vps34$^{f/f}$Lck-cre T lymphocytes. Both types of T lymphocytes undergo apoptosis. However, autophagy-deficient T lymphocytes have increased mitochondria, elevated ROS production and Bcl-2 expression, and normal IL-7Rα surface expression (9, 11). This phenotype in autophagy-deficient T cells is caused by a failure in clearance of excess mitochondria when thymocytes exit to the periphery, consistent with an essential role for autophagy to regulate intracellular organelle homeostasis. In contrast, Vps34$^{f/f}$Lck-cre T cells do not have detectable defects in mitochondria clearance. These results suggest that Vps34 is either not involved or functionally compensated for in the autophagy induction pathway by other molecules in T lymphocytes, perhaps even by other classes of PI3Ks or degradation products of PI3K class I substrates. The ability of 3-methyladenine to successfully limit autophagy induction in T lymphocytes would indicate that Vps34 and class I/II PI3K are all involved in this process, either in compensating for Vps34 kinase activity, contributing to PI3K

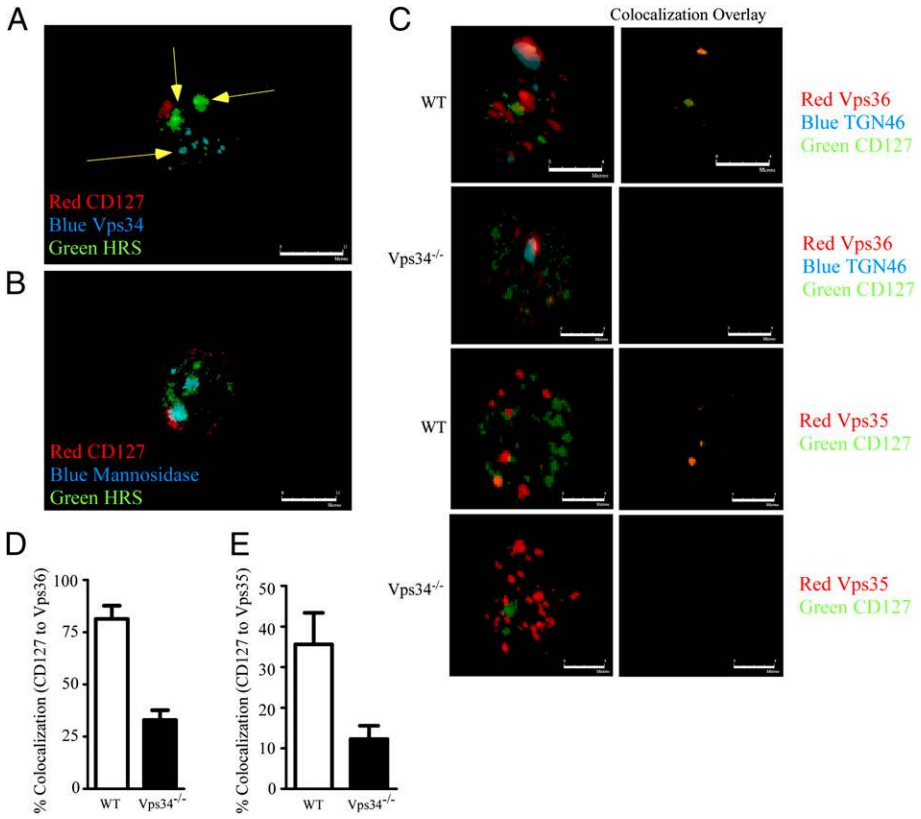

FIGURE 6. Internalized IL-7Rα localizes primarily within Vps36 vesicles. Freshly isolated T cells were fixed, permeabilized, and stained with indicated Abs for fluorescence microscopy. *A*, Vps34 colocalizes with HRS in MVB. *B*, IL-7Rα is enriched near the Golgi apparatus. *C*, Vps36 colocalizes with IL-7Rα intracellularly, and to a lesser extent, with TGN46 in WT T cells. *D*, Quantification of IL-7Rα and Vps36 colocalization (n = 20). *E*, Colocalization between IL-7Rα and Vps35 (n = 20). Data are representative of two experiments. *C–E*, Vps34$^{-/-}$ = ps34$^{f/f}$Lck-cre.

scaffolding, or by generating higher ordered phosphatidylinositol phosphate substrates that could be devolved to PI(3)P.

The inability to maintain IL-7Rα surface expression on Vps34$^{f/f}$ Lck-cre T cells likely plays a predominant role in their increased apoptosis. Consistent with the lowered IL-7Rα surface expression, Vps34$^{f/f}$Lck-cre T cells have lowered expression of Bcl-2 and defective signaling as reflected by reduced phospho-Stat5 upon IL-7 stimulation. Interestingly, Mcl-1, another member of the Bcl-2 family that is critical for naive T cell survival, is expressed at a higher level in Vps34$^{f/f}$Lck-cre T cells than that in control T cells. This result suggests that Mcl-1 may be subjected to additional level of regulation that depends on Vps34. Nevertheless, IL-7Rα–mediated signaling to promote T cell survival is not just restricted to its role in promoting the expression of the anti-apoptotic Bcl-2 family members (2). IL-7R stimulation also activates PI3K–AKT–mammalian target of rapamycin pathway and sustains expression of the glucose transporter GLUT1 (37). Thus, transgenic expression of Bcl-2 can only partially rescue the T cell defect in IL-7Rα–deficient mice (38, 39). Consistent with this, crossing of Vps34$^{f/f}$Lck-cre mice to a Bcl-2 transgenic line only partially rescued the defective T cell compartment. Interestingly, deletion of Bim did not have any rescuing effect on the T cell compartment in Vps34$^{f/f}$Lck-cre mice. This is in sharp contrast to a near normal T cell compartment in IL-7Rα$^{-/-}$Bim$^{-/-}$

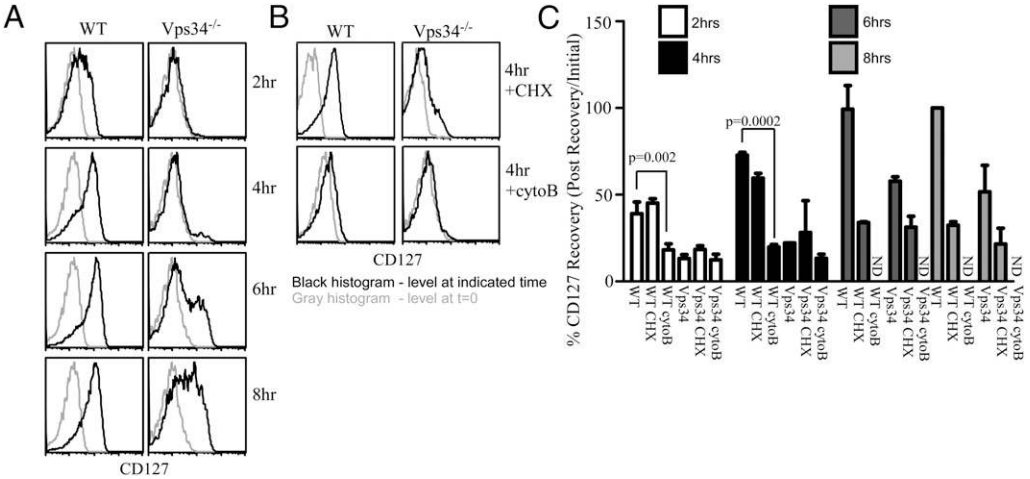

FIGURE 7. Defective IL-7Rα recovery in Vps34$^{f/f}$Lck-cre T cells that is dependent on vesicle trafficking. *A*, IL-7Rα expression on Vps34$^{f/f}$Lck-cre T cells postpronase treatment. Vps34$^{f/f}$Lck-cre CD4^{+} T cells were treated twice with 0.08% pronase for 15 min, washed, and allowed to recover for indicated times, in the presence or absence (*B*) of cycloheximide (CHX) or cytochalasin B (cytoB). Grey histograms represent IL-7Rα surface levels at time 0, immediately after pronase treatment, which is indicative of pronase efficacy. *C*, Values from *A* and *B* are calculated, normalized to starting IL-7Rα surface expression; n = 4. Data are representative of two independent experiments. *A–C*, Vps34$^{-/-}$ = Vps34$^{f/f}$Lck-cre.

mice (40). This result strongly suggests that $Vps34^{f/f}$Lck-cre T cells have additional defect that is not caused by the lowered surface expression of IL-7Rα. This is in agreement with the profound effect seen on DP cells, which do not express IL-7Rα, yet still succumb to apoptosis. Although the deletion efficiency in more mature populations was >80% (Supplemental Fig. 1), the remaining DP cells still had 75% of WT Vps34 protein levels. This is consistent with a long half-life of Vps34 protein and suggests that as Vps34 is gradually deleted in developing $Vps34^{f/f}$ Lck-cre thymocytes, more mature T lineage cells die of a progressive Vps34 loss. Because the developing DP thymocytes were not synchronized, it remains possible that the loss of Vps34 in DP thymocytes was not synchronous and that thymocytes, which lost Vps34 earlier in development, were the first victims of apoptosis. However, those DP thymocytes, which deleted Vps34 later in development, could have produced or scavenged PI(3)P at levels sufficient to maintain cell viability.

Our results have also suggested a clear route for normal IL-7Rα intracellular trafficking. Under steady-state conditions, IL-7Rα that has not been bound to a ligand is internalized and returned to the surface through homeostatic recycling (8). IL-7R internalized by the cell is sorted via the early endosome into the multivesicular body. The internalized receptor proteins are shuttled through the network of MVB compartments, and our data show ESCRT-0 and ESCRT-II seem to be distinctly located within the network. Some of the receptor under optimally signaled conditions will be destined for the late endosome and, ultimately, the lysosome (7). However, during the MVB to late-endosomal transition, Vps34 activity can save the IL-7Rα-chain from destruction for a retrograde endosomal to Golgi translocation for surface re-expression. It is likely that this MVB to late-endosomal transition is the rate-limiting step in this whole process, because we observed a majority of the internalized IL-7Rα within the Vps36 compartment, but not the HRS-bearing compartment, after taking the cells from an IL-7–rich environment in vivo and starving them.

This process appears to be disrupted in the absence of Vps34 at several stages. First, Vps34 has a profound effect on the localization and maturation of HRS-containing multivesicular bodies. This early ESCRT protein has been shown to regulate the fate of Na^+ channel by binding to the ubiquitinated form and either targeting it for degradation or shuttling it into a later cell surface recycling pattern (24). The HRS-containing ESCRT-0 complex is generally thought to cluster ubiquitinated cargoes for further intralumenal vesicle formation (41), and we observe a striking aggregation of this complex in the MVB of T cells lacking Vps34.

Second, Vps34 deficiency disrupts the localization of Vps36, which contains a GLUE domain. This protein functions as part of the ESCRT-II complex, which has been shown to be important for membrane invagination and budding of ubiquitin positive-containing intralumenal vesicles (41). The consequence of this mislocalization likely accounts for not only the inability of IL-7Rα to enter the late-endosomal to retromer pathway but also accounts for the inability for internalized IL-7 to be properly targeted to lysosome. In the absence of Vps34, internalized IL-7Rα might be either mislocalized within abnormal Eea1-negative early endosomes (42), or in HRS negative early MVB compartments, that are unable to further mature without PI(3)P and become aggregated intracellularly. The alternative intracellular sorting pathway in the absence of Vps34 kinase activity remains to be determined.

Finally, it has been shown that Vps34 has a profound effect on the localization of Eea1, which contains the eponymous FYVE domain, in the early endosome, synergizing with Rab5 (42). This interaction has been proposed to be necessary for both endosomal membrane fusion within the early endosomal compartment, as well as providing an inward directionality to vesicle transport (42). However, internalization of IL-7Rα is intact in the absence of Vps34, and the surface levels of many other receptors, which undoubtedly require unique sorting mechanisms, are normal in $Vps34^{f/f}$Lck-cre T cells.

Ideally, in a clinical setting, pharmacological inhibition or enhancement of Vps34activity could be used to "tune" the amount of prosurvival receptors in various pathogenic settings. If IL-7Rα surface expression can be modulated, allowing for maximal numbers of T lymphocytes to be sustained off highly limited amounts of growth factors, then the repertoire of polyclonal naive $CD4^+$ T cells can be maintained or diversified into old age. In addition, the amounts and clonalities of memory responses might be modulated in this manner, as IL-7Rα has been implicated as a marker for memory cell precursors. This would suggest that Vps34 is a highly attractive candidate for therapeutic intervention in preventing or modulating various lymphopenic conditions.

Acknowledgments

We thank Dr. Jeff Rathmell for the thoughtful reading and advice on the manuscript.

Disclosures

The authors have no financial conflicts of interest.

References

1. Plas, D. R., J. C. Rathmell, and C. B. Thompson. 2002. Homeostatic control of lymphocyte survival: potential origins and implications. *Nat. Immunol.* 3: 515–521.
2. Takada, K., and S. C. Jameson. 2009. Naive T cell homeostasis: from awareness of space to a sense of place. *Nat. Rev. Immunol.* 9: 823–832.
3. Fry, T. J., and C. L. Mackall. 2005. The many faces of IL-7: from lymphopoiesis to peripheral T cell maintenance. *J. Immunol.* 174: 6571–6576.
4. He, Y. W., and T. R. Malek. 1998. The structure and function of γc-dependent cytokines and receptors: regulation of T lymphocyte development and homeostasis. *Crit. Rev. Immunol.* 18: 503–524.
5. Mazzucchelli, R., and S. K. Durum. 2007. Interleukin-7 receptor expression: intelligent design. *Nat. Rev. Immunol.* 7: 144–154.
6. Park, J. H., Q. Yu, B. Erman, J. S. Appelbaum, D. Montoya-Durango, H. L. Grimes, and A. Singer. 2004. Suppression of IL7Rα transcription by IL-7 and other prosurvival cytokines: a novel mechanism for maximizing IL-7–dependent T cell survival. *Immunity* 21: 289–302.
7. Henriques, C. M., J. Rino, R. J. Nibbs, G. J. Graham, and J. T. Barata. 2010. IL-7 induces rapid clathrin-mediated internalization and JAK3-dependent degradation of IL-7Rα in T cells. *Blood* 115: 3269–3277.
8. Faller, E. M., S. M. Sugden, M. J. McVey, J. A. Kakal, and P. A. MacPherson. 2010. Soluble HIV Tat protein removes the IL-7 receptor α-chain from the surface of resting CD8 T cells and targets it for degradation. *J. Immunol.* 185: 2854–2866.
9. Pua, H. H., I. Dzhagalov, M. Chuck, N. Mizushima, and Y. W. He. 2007. A critical role for the autophagy gene Atg5 in T cell survival and proliferation. *J. Exp. Med.* 204: 25–31.
10. Levine, B., and D. J. Klionsky. 2004. Development by self-digestion: molecular mechanisms and biological functions of autophagy. *Dev. Cell* 6: 463–477.
11. Pua, H. H., J. Guo, M. Komatsu, and Y. W. He. 2009. Autophagy is essential for mitochondrial clearance in mature T lymphocytes. *J. Immunol.* 182: 4046–4055.
12. Kanki, T., and D. J. Klionsky. 2010. The molecular mechanism of mitochondria autophagy in yeast. *Mol. Microbiol.* 75: 795–800.
13. Petiot, A., E. Ogier-Denis, E. F. Blommaart, A. J. Meijer, and P. Codogno. 2000. Distinct classes of phosphatidylinositol 3′-kinases are involved in signaling pathways that control macroautophagy in HT-29 cells. *J. Biol. Chem.* 275: 992–998.
14. Kihara, A., T. Noda, N. Ishihara, and Y. Ohsumi. 2001. Two distinct Vps34 phosphatidylinositol 3-kinase complexes function in autophagy and carboxypeptidase Y sorting in *Saccharomyces cerevisiae*. *J. Cell Biol.* 152: 519–530.
15. Stack, J. H., P. K. Herman, P. V. Schu, and S. D. Emr. 1993. A membrane-associated complex containing the Vps15 protein kinase and the Vps34 PI 3-kinase is essential for protein sorting to the yeast lysosome-like vacuole. *EMBO J.* 12: 2195–2204.
16. Backer, J. M. 2008. The regulation and function of Class III PI3Ks: novel roles for Vps34. *Biochem. J.* 410: 1–17.
17. Zeng, X., J. H. Overmeyer, and W. A. Maltese. 2006. Functional specificity of the mammalian Beclin-Vps34 PI 3-kinase complex in macroautophagy versus endocytosis and lysosomal enzyme trafficking. *J. Cell Sci.* 119: 259–270.

18. Kihara, A., Y. Kabeya, Y. Ohsumi, and T. Yoshimori. 2001. Beclin-phosphatidylinositol 3-kinase complex functions at the trans-Golgi network. *EMBO Rep.* 2: 330–335.
19. Sun, Q., W. Fan, K. Chen, X. Ding, S. Chen, and Q. Zhong. 2008. Identification of Barkor as a mammalian autophagy-specific factor for Beclin 1 and class III phosphatidylinositol 3-kinase. *Proc. Natl. Acad. Sci. USA* 105: 19211–19216.
20. Zhong, Y., Q. J. Wang, X. Li, Y. Yan, J. M. Backer, B. T. Chait, N. Heintz, and Z. Yue. 2009. Distinct regulation of autophagic activity by Atg14L and Rubicon associated with Beclin 1-phosphatidylinositol-3-kinase complex. *Nat. Cell Biol.* 11: 468–476.
21. Takahashi, Y., D. Coppola, N. Matsushita, H. D. Cualing, M. Sun, Y. Sato, C. Liang, J. U. Jung, J. Q. Cheng, J. J. Mulé, et al. 2007. Bif-1 interacts with Beclin 1 through UVRAG and regulates autophagy and tumorigenesis. *Nat. Cell Biol.* 9: 1142–1151.
22. Schu, P. V., K. Takegawa, M. J. Fry, J. H. Stack, M. D. Waterfield, and S. D. Emr. 1993. Phosphatidylinositol 3-kinase encoded by yeast VPS34 gene essential for protein sorting. *Science* 260: 88–91.
23. Herman, P. K., and S. D. Emr. 1990. Characterization of VPS34, a gene required for vacuolar protein sorting and vacuole segregation in *Saccharomyces cerevisiae*. *Mol. Cell. Biol.* 10: 6742–6754.
24. Zhou, X., L. Wang, H. Hasegawa, P. Amin, B. X. Han, S. Kaneko, Y. He, and F. Wang. 2010. Deletion of PIK3C3/Vps34 in sensory neurons causes rapid neurodegeneration by disrupting the endosomal but not the autophagic pathway. *Proc. Natl. Acad. Sci. USA* 107: 9424–9429.
25. Hennet, T., F. K. Hagen, L. A. Tabak, and J. D. Marth. 1995. T-cell–specific deletion of a polypeptide *N*-acetylgalactosaminyl-transferase gene by site-directed recombination. *Proc. Natl. Acad. Sci. USA* 92: 12070–12074.
26. Funderburk, S. F., Q. J. Wang, and Z. Yue. 2010. The Beclin 1-VPS34 complex —at the crossroads of autophagy and beyond. *Trends Cell Biol.* 20: 355–362.
27. Zhang, N., H. Hartig, I. Dzhagalov, D. Draper, and Y. W. He. 2005. The role of apoptosis in the development and function of T lymphocytes. *Cell Res.* 15: 749–769.
28. Futter, C. E., L. M. Collinson, J. M. Backer, and C. R. Hopkins. 2001. Human VPS34 is required for internal vesicle formation within multivesicular endosomes. *J. Cell Biol.* 155: 1251–1264.
29. Hémar, A., A. Subtil, M. Lieb, E. Morelon, R. Hellio, and A. Dautry-Varsat. 1995. Endocytosis of interleukin 2 receptors in human T lymphocytes: distinct intracellular localization and fate of the receptor α, β, and γ chains. *J. Cell Biol.* 129: 55–64.
30. Williams, R. L., and S. Urbé. 2007. The emerging shape of the ESCRT machinery. *Nat. Rev. Mol. Cell Biol.* 8: 355–368.
31. Katzmann, D. J., M. Babst, and S. D. Emr. 2001. Ubiquitin-dependent sorting into the multivesicular body pathway requires the function of a conserved endosomal protein sorting complex, ESCRT-I. *Cell* 106: 145–155.
32. Nothwehr, S. F., S. A. Ha, and P. Bruinsma. 2000. Sorting of yeast membrane proteins into an endosome-to-Golgi pathway involves direct interaction of their cytosolic domains with Vps35p. *J. Cell Biol.* 151: 297–310.
33. Tabuchi, M., T. Yoshimori, K. Yamaguchi, T. Yoshida, and F. Kishi. 2000. Human NRAMP2/DMT1, which mediates iron transport across endosomal membranes, is localized to late endosomes and lysosomes in HEp-2 cells. *J. Biol. Chem.* 275: 22220–22228.
34. Park, J. H., S. Adoro, P. J. Lucas, S. D. Sarafova, A. S. Alag, L. L. Doan, B. Erman, X. Liu, W. Ellmeier, R. Bosselut, et al. 2007. 'Coreceptor tuning': cytokine signals transcriptionally tailor CD8 coreceptor expression to the self-specificity of the TCR. [see comment] *Nat. Immunol.* 8: 1049–1059.
35. Domen, J., K. L. Gandy, and I. L. Weissman. 1998. Systemic overexpression of BCL-2 in the hematopoietic system protects transgenic mice from the consequences of lethal irradiation. *Blood* 91: 2272–2282.
36. Engelman, J. A., J. Luo, and L. C. Cantley. 2006. The evolution of phosphatidylinositol 3-kinases as regulators of growth and metabolism. *Nat. Rev. Genet.* 7: 606–619.
37. Wofford, J. A., H. L. Wieman, S. R. Jacobs, Y. Zhao, and J. C. Rathmell. 2008. IL-7 promotes Glut1 trafficking and glucose uptake via STAT5-mediated activation of Akt to support T-cell survival. *Blood* 111: 2101–2111.
38. Maraskovsky, E., L. A. O'Reilly, M. Teepe, L. M. Corcoran, J. J. Peschon, and A. Strasser. 1997. Bcl-2 can rescue T lymphocyte development in interleukin-7 receptor-deficient mice but not in mutant rag-$1^{-/-}$ mice. *Cell* 89: 1011–1019.
39. Akashi, K., M. Kondo, U. von Freeden-Jeffry, R. Murray, and I. L. Weissman. 1997. Bcl-2 rescues T lymphopoiesis in interleukin-7 receptor-deficient mice. *Cell* 89: 1033–1041.
40. Pellegrini, M., P. Bouillet, M. Robati, G. T. Belz, G. M. Davey, and A. Strasser. 2004. Loss of Bim increases T cell production and function in interleukin 7 receptor-deficient mice. *J. Exp. Med.* 200: 1189–1195.
41. Wollert, T., and J. H. Hurley. 2010. Molecular mechanism of multivesicular body biogenesis by ESCRT complexes. *Nature* 464: 864–869.
42. Simonsen, A., R. Lippé, S. Christoforidis, J. M. Gaullier, A. Brech, J. Callaghan, B. H. Toh, C. Murphy, M. Zerial, and H. Stenmark. 1998. EEA1 links PI(3)K function to Rab5 regulation of endosome fusion. *Nature* 394: 494–498.